

Spin-Orbit Coupling in an f-electron Tight-Binding Model

M. D. Jones

*Department of Physics and Center for Computational Research,
University at Buffalo, The State University of New York, Buffalo, NY 14260**

R. C. Albers

*Theoretical Division, Los Alamos National Laboratory,
Los Alamos, NM 87501[†]*

(Dated: February 10, 2022)

We extend a tight-binding method to include the effects of spin-orbit coupling, and apply it to the study of the electronic properties of the actinide elements Th, U, and Pu. These tight-binding parameters are determined for the fcc crystal structure using the equivalent equilibrium volumes. In terms of the single particle energies and the electronic density of states, the overall quality of the tight-binding representation is excellent and of the same quality as without spin-orbit coupling. The values of the optimized tight-binding spin-orbit coupling parameters are comparable to those determined from purely atomic calculations.

PACS numbers: 71.15.Ap, 71.15.Nc, 71.15.Rf, 71.20.Gj, 71.70.Ej

I. INTRODUCTION

The accurate determination of inter-atomic forces is crucial for almost all aspects of modeling the fundamental behavior of materials. Whether one is interested in static equilibrium properties using Monte Carlo methods, or time dependent phenomena using molecular dynamics, the essential feature remains the origin, applicability, and transferability of the forces acting on the fundamental unit being modeled (atoms or molecules in most cases). First principles methods based on density functional theory have gained wide acceptance for their ease of use, relatively accurate determination of fundamental properties, and high transferability. These techniques, however, are limited in their application by current computing technology to systems of a few hundred atoms or less (most commonly a few dozen atoms). Potentials that are classically derived (i.e., pair potentials) lack directional bonding (or at best add some bond angle information) and other quantum mechanical effects but are computationally far more tractable for larger simulations. Recent advances in tight-binding (TB) theory, which include directional bonding, but treat only the most important valence electrons shells, therefore show a great deal of promise.

TB models have become a useful method for the computational modeling of materials properties thanks to their ability to incorporate quantum mechanics in a greatly simplified theoretical treatment, making large accurate simulations possible on modern digital computers^{1,2}. Another advantage of these TB models is their ability to treat a general class of problems that include directional bonding between valence electrons, of particular importance for transition metal and *f*-electron materials. Finally, TB models are widely used in many-body formalisms for the one-electron part of the Hamiltonian. It is therefore a useful representation of the band-structure for a more sophisticated treatment of electronic

correlation, and has so been used³, for example, in dynamical mean-field theory applications for Pu.

In this report we present recent developments towards a transferable tight-binding total energy technique applicable to heavy metals. With the addition of spin-orbit coupling effects for angular momentum up to (and including) *f*-character, we demonstrate the applicability of this technique for the element Pu, of particular interest for its position near the half-filling point of the 5*f* sub-shell in the actinide sequence and the boundary between localized and delocalized *f*-electrons⁴.

II. TB METHOD

The TB model used in this report is similar to that used in the handbook by Papaconstantopoulos⁵. We have extended the calculations to include *f*-electrons⁶ and spin-orbit coupling⁷. As such, in this report we will elaborate only on those aspects of the technique that are unique to this work. A very brief recapitulation of the underlying TB method and its approximations is included to create the proper context for the addition of *f*-electrons and spin-orbit coupling.

The Slater-Koster method⁸ consists of solving the secular equation,

$$H\psi_{i,v} = \epsilon_{i,v}S\psi_{i,v}, \quad (1)$$

for the single-particle eigenvalues and orbitals, under the following restrictions: terms involving more than two centers are ignored, terms where the orbitals are on the same atomic site are taken as constants, and the resulting reduced set of matrix elements are treated as variable parameters. The Hamiltonian, H , includes the labels for orbitals having generic quantum numbers α, β localized on atoms i, j , where the effective potential is assumed to be spherical, and can be represented as a sum over

atomic centers,

$$H_{\alpha i, \beta j} = \left\langle \alpha, i \left| -\nabla^2 + \sum_k V_k^{\text{eff}} \right| \beta, j \right\rangle, \quad (2)$$

which we further decompose into “on-site” and “inter-

site” terms,

$$H_{\alpha i, \beta j} = e_{\alpha} \delta_{\alpha\beta} \delta_{ij} + E_{\alpha i, \beta j \neq i}, \quad (3)$$

where the on-site terms, e_{α} , represent terms in which two orbitals share the same atomic site, and

$$E_{\alpha i, \beta j \neq i} = \sum_n e^{i\mathbf{k} \cdot (\mathbf{R}_n + \mathbf{b}_j - \mathbf{b}_i)} \int d\mathbf{r} \psi_{\alpha}(\mathbf{r} - \mathbf{R}_n - \mathbf{b}_i) H \psi_{\beta}(\mathbf{r} - \mathbf{b}_j), \quad (4)$$

are the remaining energy integrals involving orbitals located on different atomic sites, and we have used translational invariance to reduce the number of sums over bravais lattice points $\{\mathbf{R}_n\}$, and the \mathbf{b}_i denote atomic basis vectors within the repeated lattice cells. Note that terms which have both orbitals located on the same site, but the effective potential (V^{eff}) on other sites have been ignored. These contributions are typically taken to be “environmental” corrections to the on-site terms, and are not accounted for in the usual Slater-Koster formalism. For the inter-site terms, the two center approximation also consists of ignoring these additional terms in which the effective potential, V^{eff} , does not lie on one of the atomic sites. Once this approximation has been made, the inter-atomic ($i \neq j$) matrix elements reduce to a simple sum over angular functions, $G_{ll'm}(\Omega_{i,j})$, and functions which depend only upon the magnitude of the distances between atoms,

$$H_{\alpha i, \beta j} = \sum h_{ll'm}(r_{ij}) G_{ll'm}(\Omega_{i,j}), \quad (5)$$

where we have now adopted the usual convention of using the familiar l, m angular momentum quantum numbers, and the axis connecting the atoms is the quantization axis. An equivalent expression for $s_{ll'm}$ terms exists when non-orthogonal orbitals are used. The basis set used for the α and β quantum states are the cubic harmonics⁹ whose functional forms are given in Table I (with appropriate normalization factors) where $|\pm\rangle$ denotes the spin-state, which we will need for spin-orbit coupling.

The Slater-Koster tables for the sp^3d^5 matrix elements can be found in standard references¹⁰, and we have used the tabulated results of Takegahara *et al.*¹¹ for the additional matrix elements involving f -electrons. Typical TB applications are then reduced to using TB as an interpolation scheme; the matrix elements ($h_{ll'm}$, $s_{ll'm}$ and e_{α}) are determined by fitting to *ab-initio* calculated quantities such as the total energy and band energies.

In this study we restrict ourselves to the determination of optimal TB parameters at the neighbor distances in the face-centered cubic crystal structure (often used as a surrogate for the more complex ground state crystal structure of the actinides) near the equilibrium volume.

Such tabulations have been extensively used⁵ in the study of materials with lower atomic number. To the best of our knowledge this is the first time that such parameters have been presented for light actinide elements that include the f -electron orbitals (although similar parameters have been determined for the elements Ac and Th in an sp^3d^5 basis⁵). The TB parameter values so derived are available (on request) from the authors.

A. Spin-orbit coupling

The primary impact of spin-orbit coupling is to non-trivially couple electrons of different spin states, thus doubling the size of the TB Hamiltonian. The spin-orbit contribution to the Hamiltonian is given by

$$H^{so} = \xi(r) \mathbf{L} \cdot \mathbf{S}, \quad (6)$$

where $\xi(r) = (\alpha^2/(2r))(\partial V/\partial r)$, V is the total (crystal) potential. We neglect contributions from more than one center. A new Hamiltonian matrix can then be defined in terms of the spinless one,

$$\mathcal{H} = H + H^{so} = \begin{pmatrix} H + \frac{1}{2}\xi L_z & \frac{1}{2}\xi L_- \\ \frac{1}{2}\xi L_+ & H - \frac{1}{2}\xi L_z \end{pmatrix} \quad (7)$$

where

$$\xi_{nl} = \hbar \int_0^{\infty} \xi(r) [R_{nl}^0(r)]^2 r^2 dr, \quad (8)$$

is the spin-orbit coupling parameter between orbitals of orbital angular momentum l and primary quantum number n located on the same atom, L_{\pm} are the usual raising and lowering operators, and L_z the azimuthal angular momentum operator,

$$\begin{aligned} L_{\pm} Y_{lm}(\theta, \phi) &= \hbar \sqrt{l(l+1) - m(m \pm 1)} Y_{lm \pm 1} \\ L_z Y_{lm}(\theta, \phi) &= \hbar m Y_{lm}. \end{aligned}$$

The functions $R_{nl}^0(r)$ are the non-relativistic radial wave functions. The spin-orbit contributions to the Hamiltonian matrix can then be expressed in term of the TB

TABLE I: TB basis functions used for an $sp^3d^5f^7$ calculation. Note that $f_l(r) = 1/r^l$.

| $l=0$ | $l=1$ | $l=2$ | $l=3$ |
|---|---|---|---|
| $ s\pm\rangle = \frac{1}{\sqrt{4\pi}} \pm\rangle$ | $ p_1\pm\rangle = \frac{\sqrt{3}}{\sqrt{4\pi}}f_1(r)x \pm\rangle$ $ p_2\pm\rangle = \frac{\sqrt{3}}{\sqrt{4\pi}}f_1(r)y \pm\rangle$ $ p_3\pm\rangle = \frac{\sqrt{3}}{\sqrt{4\pi}}f_1(r)z \pm\rangle$ | $ d_1\pm\rangle = \frac{\sqrt{5}}{\sqrt{16\pi}}f_2(r)xy \pm\rangle$ $ d_2\pm\rangle = \frac{2\sqrt{15}}{\sqrt{16\pi}}f_2(r)yz \pm\rangle$ $ d_3\pm\rangle = \frac{2\sqrt{15}}{\sqrt{16\pi}}f_2(r)zx \pm\rangle$ $ d_4\pm\rangle = \frac{\sqrt{15}}{\sqrt{16\pi}}f_2(r)(x^2 - y^2) \pm\rangle$ $ d_5\pm\rangle = \frac{\sqrt{5}}{\sqrt{16\pi}}f_2(r)(3z^2 - r^2) \pm\rangle$ | $ f_1\pm\rangle = \frac{2\sqrt{105}}{\sqrt{16\pi}}f_3(r)xyz \pm\rangle$ $ f_2\pm\rangle = \frac{\sqrt{7}}{\sqrt{16\pi}}f_3(r)x(5x^2 - 3r^2) \pm\rangle$ $ f_3\pm\rangle = \frac{\sqrt{7}}{\sqrt{16\pi}}f_3(r)y(5y^2 - 3r^2) \pm\rangle$ $ f_4\pm\rangle = \frac{\sqrt{7}}{\sqrt{16\pi}}f_3(r)z(5z^2 - 3r^2) \pm\rangle$ $ f_5\pm\rangle = \frac{\sqrt{105}}{\sqrt{16\pi}}f_3(r)x(y^2 - z^2) \pm\rangle$ $ f_6\pm\rangle = \frac{\sqrt{105}}{\sqrt{16\pi}}f_3(r)y(z^2 - x^2) \pm\rangle$ $ f_7\pm\rangle = \frac{\sqrt{105}}{\sqrt{16\pi}}f_3(r)z(x^2 - y^2) \pm\rangle$ |

basis functions listed in Table I. Rather than list contributions for the 32x32 matrix, here we list the matrices in the sub-blocks corresponding to each orbital angular momentum. The p and d contributions have been previously discussed in relation to the tight-binding formalism^{12,13};

to the best of our knowledge no f contribution has yet appeared in the literature. For completeness we detail the spin-orbit contribution for all values of the angular momentum up to $l = 3$.

$$H_p^{so} = \frac{\xi_{np}}{2} \begin{pmatrix} 0 & -i & 0 & 0 & 0 & 1 \\ i & 0 & 0 & 0 & 0 & -i \\ 0 & 0 & 0 & -1 & i & 0 \\ 0 & 0 & -1 & 0 & i & 0 \\ 0 & 0 & -i & -i & 0 & 0 \\ 1 & i & 0 & 0 & 0 & 0 \end{pmatrix}, \quad (9)$$

$$H_d^{so} = \frac{\xi_{nd}}{2} \begin{pmatrix} 0 & 0 & 0 & 2i & 0 & 0 & 1 & -i & 0 & 0 \\ 0 & 0 & i & 0 & 0 & -1 & 0 & 0 & -i & -i\sqrt{3} \\ 0 & -i & 0 & 0 & 0 & i & 0 & 0 & -1 & \sqrt{3} \\ -2i & 0 & 0 & 0 & 0 & 0 & i & 1 & 0 & 0 \\ 0 & 0 & 0 & 0 & 0 & 0 & i\sqrt{3} & -\sqrt{3} & 0 & 0 \\ 0 & -1 & -i & 0 & 0 & 0 & 0 & 0 & -2i & 0 \\ 1 & 0 & 0 & -i & -i\sqrt{3} & 0 & 0 & -i & 0 & 0 \\ i & 0 & 0 & 1 & -\sqrt{3} & 0 & i & 0 & 0 & 0 \\ 0 & i & -1 & 0 & 0 & 2i & 0 & 0 & 0 & 0 \\ 0 & i\sqrt{3} & \sqrt{3} & 0 & 0 & 0 & 0 & 0 & 0 & 0 \end{pmatrix}, \quad (10)$$

$$H_f^{so} = \frac{\xi_{nf}}{4} \begin{pmatrix} 0 & 0 & 0 & 0 & 0 & 0 & 2i & 0 & 0 & 0 & 0 & 2i & 2 & 0 \\ 0 & 0 & \frac{3i}{2} & 0 & 0 & it & 0 & 0 & 0 & 0 & -\frac{3}{2} & 0 & 0 & t \\ 0 & -\frac{3i}{2} & 0 & 0 & it & 0 & 0 & 0 & 0 & 0 & \frac{3i}{2} & 0 & 0 & it \\ 0 & 0 & 0 & 0 & 0 & 0 & 0 & 0 & \frac{3}{2} & -\frac{3i}{2} & 0 & t & it & 0 \\ 0 & 0 & -it & 0 & 0 & -\frac{i}{2} & 0 & -2i & 0 & 0 & -t & 0 & 0 & \frac{1}{2} \\ 0 & -it & 0 & 0 & \frac{i}{2} & 0 & 0 & -2 & 0 & 0 & -it & 0 & 0 & -\frac{i}{2} \\ -2i & 0 & 0 & 0 & 0 & 0 & 0 & 0 & -t & -it & 0 & -\frac{1}{2} & \frac{i}{2} & 0 \\ 0 & 0 & 0 & 0 & 2i & -2 & 0 & 0 & 0 & 0 & 0 & 0 & 0 & -2i \\ 0 & 0 & 0 & \frac{3}{2} & 0 & 0 & -t & 0 & 0 & -\frac{3i}{2} & 0 & 0 & -it & 0 \\ 0 & 0 & 0 & \frac{3i}{2} & 0 & 0 & it & 0 & \frac{3i}{2} & 0 & 0 & -it & 0 & 0 \\ 0 & -\frac{3}{2} & -\frac{3i}{2} & 0 & -t & it & 0 & 0 & 0 & 0 & 0 & 0 & 0 & 0 \\ -2i & 0 & 0 & t & 0 & 0 & -\frac{1}{2} & 0 & 0 & it & 0 & 0 & \frac{i}{2} & 0 \\ 2 & 0 & 0 & -it & 0 & 0 & -\frac{i}{2} & 0 & it & 0 & 0 & -\frac{i}{2} & 0 & 0 \\ 0 & t & -it & 0 & \frac{1}{2} & \frac{i}{2} & 0 & 2i & 0 & 0 & 0 & 0 & 0 & 0 \end{pmatrix}, \quad (11)$$

where $t = \sqrt{15}/2$.

B. Fitting the Parameters

The values of the TB parameters were determined using standard non-linear least squares optimization rou-

tines by matching energy band values derived from highly accurate first principles density functional theory (DFT) calculations¹⁴. The technique is described in detail in a previous work⁶, where the DFT calculations in this case used a generalized gradient approximation DFT functional¹⁵, and the improved tetrahedron scheme¹⁶ for Brillouin zone integrations. In this study we use as a starting point high quality fits to the scalar-relativistic energy bands and approximate atomic values of the spin-orbit parameters. The first step is to then use this fit for fitting the relativistic energy bands including spin-orbit coupling. Successive optimization steps then relax only the spin-orbit coupling parameters (step 1), the remaining on-site parameters (step 2), and finally the inter-site terms (step 3). The fit quality through these steps is shown in Figure 1. Note that the quality of the final fit is comparable to the original fit quality (open symbols at step 3) when only scalar-relativistic effects were taken into account.

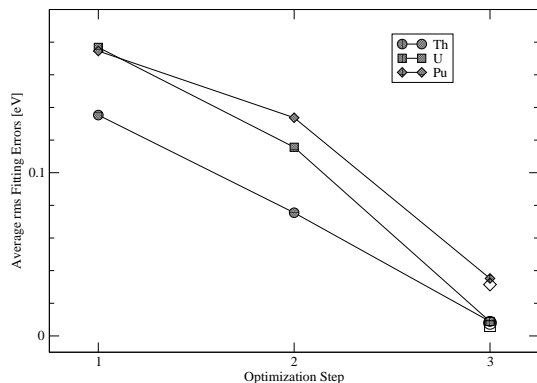


FIG. 1: TB fit quality in terms of the cumulative root mean square (rms) errors at various steps of the optimization procedure. Step 1 relaxes the spin-orbit parameters (ξ_{nl}), 2 relaxes the remaining on-site parameters, and 3 is a full relaxation of all parameters. Open symbols at Step 3 indicate the original scalar-relativistic fit quality. Note that the cumulative rms error is over all of the fitted bands (20 bands for Th, U, and Pu). Although the spin-orbit coupling is an atomic quantity, the improvement of our results in step 3 (which relaxes inter-site parameters) indicates some environmental effects should also be taken into account.

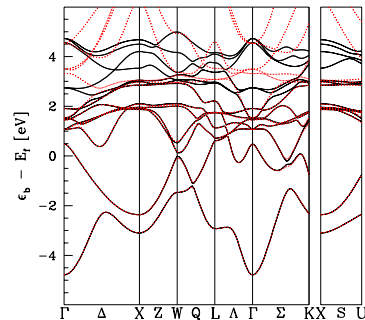
III. APPLICATION TO THE LIGHT ACTINIDES, TH, U, AND PU

A. Energy bands including spin-orbit coupling

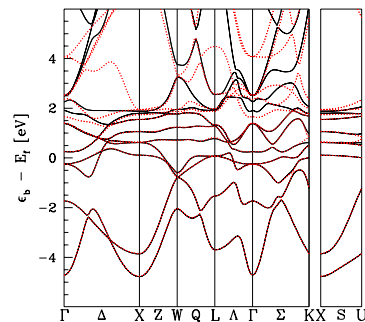
The first comparison between the TB fit and FLAPW calculations are the energy bands shown in Figure 2. Note the excellent agreement between the two sets of

calculations (the cumulative root mean square error in the TB fits to the first 20 energy bands in the irreducible Brillouin zone is 0.013, 0.013, and 0.072 Ry, respectively).

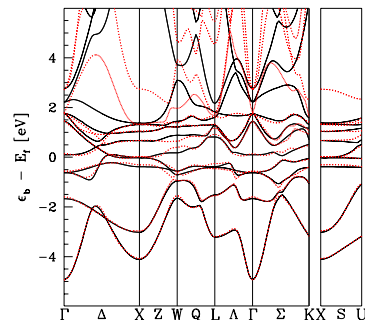
Also note that we have included the “semi-core” 6p



(a)Th



(b)U



(c)Pu

FIG. 2: TB energy bands for Th ($a = 9.61$), U ($a = 8.22$), and Pu ($a = 8.14$), shown in comparison with FLAPW valence energy bands (dotted lines). Note the excellent agreement. The abscissa for each calculation has been shifted such that the Fermi energy is at zero. Higher valence states (above the first 20) are not fit, hence the poorer fit quality well above the Fermi level.

states in the fit to better fix the available p states in the TB basis. To expand the energy scale comparing the valence bands, the fit quality for the semi-core 6p states is

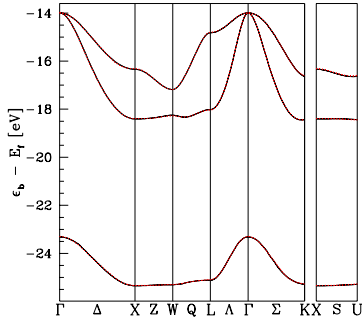


FIG. 3: TB energy bands (dashed lines) for Pu semi-core 6p states, compared with FLAPW values (solid lines).

shown separately in Figure 3 for Pu (all three elements have similar excellent fit quality for the more localized 6p states). Note that higher energy bands (well above the Fermi level) are not fit, hence the larger discrepancies for those levels.

B. Density of states including spin-orbit coupling

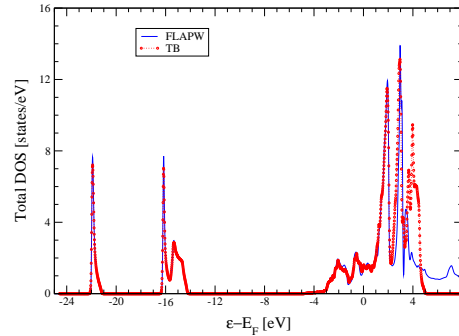
We also compare the total density of states (DOS) between TB and FLAPW methods in Figure 4.

The TB method shown in the figure used a simple Fermi-Dirac temperature smearing method (with $k_B T = 500$) for integrating over the irreducible wedge of the Brillouin zone, while the FLAPW calculations used the improved tetrahedron¹⁶ method with Gaussian smearing. From the comparison between the TB and FLAPW methods shown in the above figure, we note that the agreement is excellent, with all major features in the DOS reproduced by the TB calculations. There is a slight reduction in the height of some of the larger peaks in the DOS for the TB technique, most likely due to the inability of the temperature smearing technique to represent the finer grained features as well as the improved tetrahedron method does.

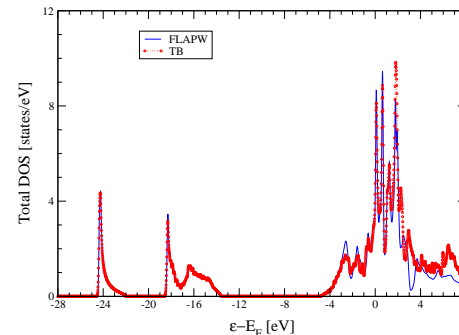
C. Spin-orbit coupling terms

It is interesting to compare the spin-orbit coupling parameters, ξ_{nl} , predicted by TB theory for the various valence shells relative to the values predicted by accurate Hartree-Fock-Slater calculations of isolated atoms¹⁹. This comparison is shown in Table II.

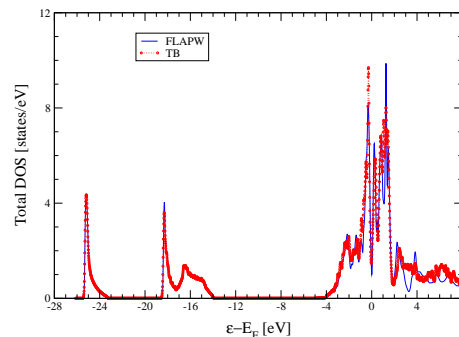
Note the overall agreement between the TB fitted parameters and the atomic values. The overall shift of a few tenths of an eV for the TB values is interesting, and this trend could be representative of crystal field effects (this speculation could be checked by performing equivalent fits at different densities). Equivalently, one can



(a)Th



(b)U



(c)Pu

FIG. 4: TB (dotted lines) and FLAPW (solid lines) total DOS, including spin-orbit coupling. Note that the TB calculation is in quite good agreement with the FLAPW results, despite using a different BZ integration method. The abscissa for each calculation has been shifted such that the Fermi energy is at zero.

compare the spin-orbit splitting of the electronic energy levels with the purely atomic case. This comparison is also shown in Table II.

TABLE II: Values of spin-orbit coupling strength, ξ_{nl} , and spin-orbit splittings, $\Delta_{nl} = (2l + 1)\xi_{nl}/2$, for the various valence electron shells predicted by the TB fit compared with purely atomic values using relativistic density functional theory (DFT)¹⁷, a Dirac-Slater atomic code (DIRAC)¹⁸, and relativistic Hartree-Fock-Slater (HFS)¹⁹ atomic calculations. Dashed entries are used for orbitals not populated in the atomic calculations. Values are in eV.

| Method | ξ_{6p} | Δ_{6p} | ξ_{5d} | | Δ_{5d} | ξ_{5f} | Δ_{5f} |
|--------|------------|---------------|------------|----|---------------|------------|---------------|
| | | | | Th | | | |
| DIRAC | 5.29 | 7.94 | 0.20 | | 0.51 | 0.19 | 0.66 |
| DFT | 5.24 | 7.86 | 0.21 | | 0.52 | — | — |
| HFS | 4.09 | 6.14 | 0.30 | | 0.75 | — | — |
| TB | 4.19 | 6.29 | 0.20 | | 0.51 | 0.18 | 0.62 |
| | | | | U | | | |
| DIRAC | 5.96 | 8.94 | 0.19 | | 0.47 | 0.24 | 0.83 |
| DFT | 5.90 | 8.85 | 0.20 | | 0.50 | 0.24 | 0.84 |
| HFS | 4.38 | 6.57 | 0.30 | | 0.75 | 0.35 | 1.24 |
| TB | 4.64 | 6.96 | 0.23 | | 0.58 | 0.42 | 1.48 |
| | | | | Pu | | | |
| DIRAC | 6.92 | 10.38 | 0.20 | | 0.51 | 0.31 | 1.10 |
| DFT | — | — | — | | — | — | — |
| HFS | 4.60 | 6.90 | — | | — | 0.41 | 1.43 |
| TB | 5.23 | 7.84 | 0.59 | | 1.46 | 0.54 | 1.90 |

IV. CONCLUSIONS

We have included f -electron and spin-orbit effects in a standard tight-binding method for solids in order to advance simpler simulation methods that are capable of the accuracy of more expensive, full-potential density-functional techniques. We have applied this TB technique to elemental fcc Th, U, and Pu, and have achieved excellent agreement with the electronic properties predicted using a highly accurate FLAPW method. The fitted spin-orbit coupling parameters match very well the values independently predicted by atomic electronic structure calculations. This methodology bodes well for further TB investigations, especially for the study of defects, phonons, and dynamical properties. In future work we intend to develop a more transferable model based on

a TB total energy formalism⁶, which should allow the straightforward calculation of detailed materials properties.

Acknowledgments

This work was carried out under the auspices of the National Nuclear Security Administration of the U.S. Department of Energy at Los Alamos National Laboratory under Contract No. DE-AC52-06NA25396. Calculations were performed at the Los Alamos National Laboratory and the Center for Computational Research at SUNY-Buffalo. FLAPW calculations were performed using the Wien2k package¹⁴. We thank Jian-Xin Zhu for providing helpful remarks.

* Electronic address: jonesm@ccr.buffalo.edu

† Electronic address: rca@lanl.gov

¹ C. M. Goringe, D. R. Bowler, and E. Hernandez, Rep. Prog. Phys. **60**, 1447 (1997).

² D. A. Papaconstantopoulos and M. J. Mehl, J. Phys.: Condens. Matter **15**, R413 (2003).

³ J.-X. Zhu, A. K. McMahan, M. D. Jones, T. Durakiewicz, J. J. Joyce, J. M. Wills, and R. C. Albers, Phys. Rev. B **76**, 245118 (2007).

⁴ R. C. Albers, Nature **410**, 759 (2001).

⁵ D. A. Papaconstantopoulos, *Handbook of the Band Structure of Elemental Solids* (Plenum Press, New York, 1986).

⁶ M. D. Jones and R. C. Albers, Phys. Rev. B **66**, 134105 (2002).

⁷ M. Lach-hab, M. J. Mehl, and D. A. Papaconstantopoulos, J. Phys. Chem. Solids **63**, 833 (2002).

⁸ J. C. Slater and G. F. Koster, Phys. Rev. **94**, 1498 (1954).

⁹ F. von Der Lage and H. A. Bethe, Phys. Rev. **71**, 612 (1947).

¹⁰ W. A. Harrison, *Electronic Structure and the Properties of Solids* (Freeman, San Francisco, CA, USA, 1980).

¹¹ K. Takegahara, Y. Aoki, and A. Yanase, J. Phys. C **13**,

583 (1980).

¹² J. Friedel, P. Lengart, and G. Leman, J. Phys. Chem. Solids **25**, 781 (1964).

¹³ D. J. Chadi, Phys. Rev. B **16**, 790 (1977).

¹⁴ P. Blaha, K. Schwarz, G. K. H. Madsen, D. Kvasnicka, and J. Luitz, *WIEN2K, An Augmented Plane Wave + Local Orbitals Program for Calculating Crystal Properties* (Karlheinz Schwartz, Techn. Universitt Wien, Austria, 2001. ISBN 3-9501031-1-2).

¹⁵ J. P. Perdew, S. Burke, and M. Ernzerhof, Phys. Rev. Lett. **77**, 3865 (1996).

¹⁶ P. E. Blöchl, O. Jepsen, and O. K. Andersen, Phys. Rev. B **49**, 16223 (1994).

¹⁷ S. Kotochigova, Z. H. Levine, E. L. Shirley, M. D. Stiles, and C. W. Clark, <http://math.nist.gov/DFTdata> (1996).

¹⁸ ADF2004.01, SCM, Theoretical Chemistry, Vrije Universiteit, Amsterdam, The Netherlands, <http://www.scm.com>.

¹⁹ F. Herman and S. Skillman, *Atomic Structure Calculations* (Prentice-Hall, Englewood Cliffs, NJ, USA, 1963).